Systematic trends of the oscillator strengths for $n=3$ and 2 electric dipole transitions in oxygenlike ions

Mau Hsiung Chen
High Temperature Physics Division, Lawrence Livermore National Laboratory, Livermore, California 94550

Bernd Crasemann
Department of Physics and Chemical Physics Institute, University of Oregon, Eugene, Oregon 97403
(Received 15 May 1989)

Energies and oscillator strengths for electric dipole transitions between states with principal quantum numbers 3 and 2 of singly excited oxygenlike ions have been calculated for 32 ions with atomic numbers $10 \le Z \le 79$ using the multiconfiguration Dirac-Fock method. The calculations include finite nuclear size, Breit interaction, and quantum electrodynamic corrections. The Z dependence of the oscillator strengths throughout the sequence is analyzed for some selected transitions. Effects of both relativity and configuration interaction are seen to be very important for medium and highly charged ions. Numerous irregularities and some sharp discontinuities in the Z dependence of the oscillator strengths are found for many transitions due to the effect of level crossings. A rapid interpolation based on results obtained for a few ionization stages can therefore lead to serious errors.

I. INTRODUCTION

Energy levels and transition probabilities of highly charged ions are important atomic parameters in the studies of atomic collisions and in the modeling of astrophysical and laboratory-produced plasmas. Analysis of systematic trends along isoelectronic sequences has proved to be a convenient and effective tool for organizing and evaluating data on oscillator strengths (f values).[1] In a normal situation, the oscillator strengths of transitions vary smoothly with atomic numer Z.[1] However, the effects of relativity, configuration interaction, and level crossing can drastically change the characteristics of oscillator strengths along an isoelectronic sequence.[2]

Relativistic calculations of transition probabilities have been carried out previously for several isoelectronic sequences.[3-8] These calculations deal mainly with transitions in which the principal quantum number does not change ($\Delta n=0$). Systematic trends of the f values for electric dipole ($E1$) transitions and the effect of level crossings on the oscillator strengths have been analyzed in detail for a few isoelectronic sequences.[2,4]

In this paper we report on a systematic relativistic calculation of x-ray energies and transition probabilities for the $E1$ transitions between states with principal quantum numbers $n=3$ and $n=2$ in the oxygen isoelectronic sequence, by means of the multiconfiguration Dirac-Fock method (MCDF).[9,10] The calculations cover 32 ions with atomic numbers $10 \le Z \le 79$ and include the transverse Breit interaction, quantum electrodynamic (QED) corrections, and finite-nuclear-size effect.[9] The Z dependence of the oscillator strengths of some selected transitions are analyzed. The effects of relativity, configuration interaction, and level crossings on the oscillator strengths are investigated.

II. THEORETICAL METHOD

In the MCDF model,[9] the configuration state functions (CSF's) denoted by $\phi(\Gamma JM)$ are formed by taking linear combinations of Slater determinants of the central field Dirac orbitals; an atomic state function (ASF) for a state i with total angular momentum JM is then constructed from CSF's:[9]

$$\psi_i(JM)=\sum_{\alpha=1}^{n} C_{i\alpha}\phi(\Gamma_\alpha JM) , \tag{1}$$

where n is the number of CSF's included in the expansion and the $C_{i\alpha}$ are the mixing coefficients for state i.

The spontaneous relativistic $E1$ transition probability for a discrete transition $i \to f$, after summation and averaging over the magnetic substates, is given in perturbation theory by[10-12]

$$W_{fi}=\frac{2\pi}{3(2J_i+1)}|\langle f\|T_1\|i\rangle|^2 . \tag{2}$$

In the MCDF method, the $E1$ reduced matrix element can be expressed in the CSF basis and then be written as a sum of products of angular factors and the one-electron reduced matrix element:[10-12]

$$\langle f\|T_1\|i\rangle=\sum_{\alpha=1}^{n_i}\sum_{\beta=1}^{n_f} C_{i\alpha}C_{f\beta}\sum_{p,q} d^1_{pq}(\beta,\alpha)\langle p\|T_1\|q\rangle , \tag{3}$$

where the $d^1_{pq}(\beta,\alpha)$ are angular factors which depend on the angular momentum and the configurational structure of the CSF;[12] the one-electron reduced matrix elements $\langle p\|T_1\|q\rangle$ are defined by Grant.[11]

In this paper the length form is used and retardation effects on the transition matrix element are included.

The absorption oscillator strength of a transition from state $|f\rangle$ to state $|i\rangle$ is given by[13]

$$f = 1.499\times 10^{-16}\frac{g_i\lambda^2 W_{fi}}{g_f} . \quad (4)$$

Here g_i and g_f are the statistical weight factors for the states $|i\rangle$ and $|f\rangle$, respectively; the wavelength λ is in Å and the radiative emission rate W_{fi} is in $\sec^{-1}$.

III. NUMERICAL CALCULATIONS

The energies and wave functions for the oxygenlike ions were calculated by the MCDF method with the average-level scheme.[9] The calculations were carried out in intermediate coupling with configuration interaction within the same complex. We used 216 CSF functions from the $2s^2 2p^3 3l$, $2s^1 2p^4 3l$, and $2s^0 2p^5 3l$ configurations for the upper states and 10 CSF functions from the $2s^2 2p^4$, $2s^1 2p^5$, and $2s^0 2p^6$ configurations for the lower levels. The mixing coefficients $C_{i\alpha}$ [Eq. (1)] were obtained by diagonalizing the energy matrix which includes Coulomb and transverse Breit interactions as well as QED corrections.

The x-ray energies were obtained by performing separate MCDF calculations for the initial and final states. However, in calculations of the transition rate, the orbital wave functions from the initial state were used and the effects of nonorthogonality between the initial and final orbital wave functions were thus neglected. The radiative $E1$ transition probabilities were calculated according to Eqs. (2) and (3) in the length gauge. The required angular factors $d^1_{pq}(\beta,\alpha)$ were calculated using a general angular momentum code for the one-electron tensor operator.[9]

IV. RESULTS AND DISCUSSION

Wavelengths and oscillator strengths for the $n=3$ and 2 $E1$ transitions of the oxygen isoelectronic sequence have been calculated for 32 ions with atomic numbers $10\le Z\le 79$ using the MCDF method. The x-ray energies and rates for the $1s^2 2s^2 2p^3 3s$-$1s^2 2s^2 2p^4$ transitions for some selected ions are listed in Table I. Complete results for all possible transitions will be published elsewhere.[14]

The energy levels for the $1s^2 2s^n 2p^m 3l$ $(n+m=5)$ and $1s^2 2s^n 2p^m$ $(n+m=6)$ configurations can be identified unambiguously by using LSJ coupling and j-j coupling notations for light and heavy ions, respectively. For medium-Z ions, it is rather difficult to classify the states consistently using the dominant component only, due to the complicated level crossings. In the present work, we use energy ordering to assist with the classification. Each energy level is identified by the LSJ coupling at low Z; it is followed through the isoelectronic sequence by using the energy ordering and nonrelativistic configuration description, and then is classified in terms of j-j coupling at high Z. Under this procedure, states with the same total angular momentum and from the same nonrelativistic configuration will not cross each other. In Table I, the same LSJ notation is retained for all ions in the oxygen isoelectronic sequence, even though it does not provide a good description for heavy ions.

Self-energy corrections in the many-electron systems are not available except for the K shell of heavy neutral atoms.[15] In the MCDF model,[9] the many-electron self-energy corrections are estimated using Mohr's point Coulomb values[16] for the $1s$, $2s$, and $2p$ levels and an n^{-3} scaling rule for the higher n levels, with an effective-charge approach to take into account the screening effect. This procedure has been found to yield good results for the $2s$-$2p$ transitions of Li-like ions while overestimating the screening effect for the $3s$-$3p$ transitions of Na-like heavy ions by ~ 0.5 eV.[17]

The contributions of the Breit interaction and QED corrections to the transition energies are displayed in Figs. 1 and 2 for two typical transitions. The Breit interaction is the dominant factor among the higher-order relativistic corrections for the $2p$-$3s$ transitions, while for the $2s$-$3p$ transitions, the self-energy correction is as large as the Breit energy for low- and medium-Z ions and becomes the dominant contributor for heavy ions. Furthermore, for precision calculations of atomic energy levels it is necessary to include the contributions from the Breit interaction and QED corrections.

In Tables II and III, the lowest $J=0$ and $J=1$ odd levels, respectively, in the $1s^2 2s^n 2p^m 3l$ $(n+m=5)$ complex of the oxygen isoelectronic sequence are listed. The levels are arranged in ascending order of energy. The energy levels are classified according to the LSJ coupling at low Z and j-j coupling at high Z. In the j-j coupling notation, the symbols l_- and l indicate the subshells with total angular momentum $j=l-\frac{1}{2}$ and $j=l+\frac{1}{2}$, respectively. Many level crossings occur along the isoelectronic sequence. These level-crossing configuration interactions can have a very significant effect on the calculation of the oscillator strengths and cause serious complications in the behavior of the oscillator strengths along the isoelectronic sequence.

Level crossing is a rather common phenomenon in the atomic-level structure of highly charged ions along an isoelectronic sequence.[2] It occurs when a spectrum restructures itself as it approaches the high-Z limit. In a relativistic calculation, effects of relativity can change the level structure and introduce many level crossings. As an example, the $1s^2 2s^2 2p^3(^2P)3s\ ^1P_1$ state goes through five level crossings with states from the $1s^2 2s^2 2p^3 3d$ configuration as Z increases from 10 to 50. The effects of level crossings on the systematic trends of the oscillator strengths for the boron, magnesium, and aluminum isoelectronic sequences have been analyzed.[2,4,5] Here, we give a few examples to illustrate the importance and frequent occurrence of level crossings in the oxygen isoelectronic sequence.

In Figs. 3–6, the oscillator strengths for some selected transitions are shown. The $2p^3 3s\ ^5S_2$–$2p^4\ ^3P_2$ and $2p^3 3d\ ^5D_1$–$2p^4\ ^3P_2$ transitions are electric dipole forbidden in the LS coupling limit and become $E1$ allowed at high Z. Thus, these $E1$ transitions are made possible by the spin-orbit interaction in low- and mid-Z ions. The oscillator strengths for these transitions increase by four orders of magnitude as Z increases from 10 to 79. The $2p^3(^2D)3s\ ^3D_3$–$2p^4\ ^3P_2$ transition is $E1$ allowed both in the low- and high-Z limits. It exhibits large oscillator

TABLE I. Calculated x-ray energies (in eV) and rates (in sec^{-1}) for the $1s^22s^22p^33s-1s^22s^22p^4$ $E1$ transitions of oxygenlike ions. (Numbers in square brackets are powers of ten.)

Final	$^3P_2$		$^3P_1$		$^3P_0$		$^1D_2$		$^1S_0$	
Initial	Energy	Rate	Energy	Rate	Energy	Rate	Energy	Rate	Energy	Rate
					Ar^{10+}					
$(^4S)^5S_2$	306.58	9.34[8]	304.79	1.77[8]			297.45	1.20[5]		
$(^4S)^3S_1$	310.89	2.55[11]	309.11	1.30[11]	308.64	4.50[10]	301.76	6.83[8]	293.02	5.09[5]
$(^2D)^3D_1$	319.85	7.72[9]	318.07	8.05[10]	317.60	5.39[10]	310.72	4.68[9]	301.98	1.15[9]
$(^2D)^3D_2$	319.91	7.12[10]	318.13	7.20[10]			310.78	6.52[8]		
$(^2D)^3D_3$	320.20	1.41[11]					311.07	2.03[9]		
$(^2D)^1D_2$	322.13	1.39[10]	320.34	8.46[9]			312.99	3.20[11]		
$(^2P)^3P_0$			324.26	1.54[11]						
$(^2P)^3P_1$	326.23	4.23[10]	324.44	3.10[10]	323.98	7.76[10]	317.10	7.82[9]	308.36	2.07[8]
$(^2P)^3P_2$	326.76	6.78[10]	324.98	6.52[10]			317.63	3.51[10]		
$(^2P)^1P_1$	328.57	8.50[8]	326.78	2.28[7]	326.31	1.52[9]	319.43	2.04[11]	310.69	1.55[11]
					Fe^{18+}					
$(^4S)^5S_2$	820.64	9.76[10]	809.59	3.74[9]			799.51	1.56[8]		
$(^4S)^3S_1$	827.16	1.95[12]	816.11	4.73[11]	817.97	3.97[11]	806.04	1.32[10]	787.34	3.10[7]
$(^2D)^3D_1$	840.54	1.59[9]	829.49	1.02[12]	831.35	1.55[11]	819.41	1.27[11]	800.72	1.50[10]
$(^2D)^3D_2$	840.26	8.23[11]	829.20	2.06[11]			819.13	8.33[10]		
$(^2D)^3D_3$	844.39	9.24[11]					823.26	8.88[10]		
$(^2D)^1D_2$	846.90	1.06[11]	835.84	2.37[11]			825.77	1.76[12]		
$(^2P)^3P_0$			843.34	9.98[11]						
$(^2P)^3P_1$	855.36	8.49[10]	844.31	1.64[11]	846.16	6.21[11]	834.23	4.75[11]	815.54	3.13[10]
$(^2P)^3P_2$	862.54	1.15[11]	851.49	5.77[11]			841.41	5.59[11]		
$(^2P)^1P_1$	864.46	2.52[10]	853.42	2.06[10]	855.28	4.85[10]	843.35	8.98[11]	824.65	1.10[12]
					Se^{26+}					
$(^4S)^5S_2$	1574.8	1.62[12]	1534.7	2.40[9]			1522.5	5.29[9]		
$(^4S)^3S_1$	1580.9	6.04[12]	1540.8	2.42[11]	1563.4	1.83[12]	1528.6	7.65[9]	1480.4	1.90[8]
$(^2D)^3D_1$	1616.1	8.91[11]	1575.9	5.07[12]	1598.5	9.51[10]	1563.7	7.65[11]	1515.6	2.06[10]
$(^2D)^3D_2$	1613.0	2.34[12]	1572.8	6.02[11]			1560.6	2.91[11]		
$(^2D)^3D_3$	1624.4	3.19[12]					1572.1	6.45[11]		
$(^2D)^1D_2$	1627.8	5.59[11]	1587.6	9.03[11]			1575.4	5.76[12]		
$(^2P)^3P_0$			1599.2	3.44[12]						
$(^2P)^3P_1$	1640.9	7.33[10]	1600.8	5.37[11]	1623.3	2.49[12]	1588.5	2.37[12]	1540.4	3.59[10]
$(^2P)^3P_2$	1674.1	1.26[11]	1634.0	2.44[12]			1621.8	2.23[12]		
$(^2P)^1P_1$	1676.7	1.11[11]	1636.6	2.46[11]	1659.2	1.01[11]	1624.4	2.71[12]	1576.2	4.16[12]
					Mo^{34+}					
$(^4S)^5S_2$	2559.1	6.46[12]	2452.1	1.33[8]			2437.9	9.69[9]		
$(^4S)^3S_1$	2564.9	1.40[13]	2458.0	9.11[10]	2539.5	5.01[12]	2443.8	2.73[9]	2327.2	9.65[7]
$(^2D)^3D_1$	2663.0	3.86[12]	2556.0	1.36[13]	2637.5	4.07[10]	2541.8	2.37[12]	2425.2	1.62[10]
$(^2D)^3D_2$	2657.3	4.76[12]	2550.4	1.74[12]			2536.2	7.30[11]		
$(^2D)^3D_3$	2673.7	9.68[12]					2552.6	2.17[12]		
$(^2D)^1D_2$	2678.1	2.18[12]	2571.2	2.21[12]			2556.9	1.44[13]		
$(^2P)^3P_0$			2587.6	8.66[12]						
$(^2P)^3P_1$	2696.4	1.80[10]	2589.5	1.31[12]	2670.9	8.39[12]	2575.3	6.59[12]	2458.7	2.24[10]
$(^2P)^3P_2$	2793.1	1.88[11]	2686.2	8.84[12]			2671.9	7.17[12]		
$(^2P)^1P_1$	2796.8	2.15[11]	2689.9	1.37[12]	2771.4	8.78[10]	2675.7	8.66[12]	2559.1	1.07[13]
					Xe^{46+}					
$(^4S)^5S_2$	4453.9	2.32[13]	4120.0	1.70[7]			4103.2	6.89[9]		
$(^4S)^3S_1$	4460.5	4.09[13]	4126.6	2.98[10]	4422.8	1.58[13]	4109.8	7.67[8]	3762.4	1.97[7]
$(^2D)^3D_1$	4782.4	9.52[12]	4448.5	4.19[13]	4744.7	2.65[12]	4431.7	8.11[12]	4084.2	9.10[9]
$(^2)^3D_2$	4774.4	1.01[12]	4440.5	6.08[12]			4423.7	2.13[12]		
$(^2D)^3D_3$	4796.2	3.85[9]					4445.5	7.95[12]		
$(^2D)^1D_2$	4801.1	3.00[12]	4467.3	6.54[12]			4450.4	4.43[13]		
$(^2P)^3P_0$			4492.4	2.67[13]						
$(^2P)^3P_1$	4829.3	4.91[11]	4495.4	4.52[12]	4791.6	5.44[12]	4478.6	2.14[13]	4131.1	9.33[9]
$(^2P)^3P_2$	5149.4	1.50[11]	4815.5	1.84[12]			4798.7	2.38[11]		
$(^2P)^1P_1$	5145.4	1.33[13]	4811.5	4.76[11]	5107.7	3.54[12]	4794.7	8.83[11]	4447.2	2.19[13]

TABLE I. (*Continued*).

Final	$^3P_2$		$^3P_1$		$^3P_0$		$^1D_2$		$^1S_0$	
Initial	Energy	Rate	Energy	Rate	Energy	Rate	Energy	Rate	Energy	Rate
					Ho^{59+}					
$(^4S)^5S_2$	7040.9	6.64[13]	6154.9	4.39[5]			6136.3	3.38[9]		
$(^4S)^3S_1$	7049.2	1.12[14]	6163.1	1.22[10]	6996.9	4.36[13]	6144.5	8.06[7]	5238.3	3.17[6]
$(^2D)^3D_1$	7921.7	3.04[13]	7035.6	1.14[14]	7869.4	2.39[11]	7017.0	2.28[13]	6110.7	4.94[9]
$(^2D)^3D_2$	7910.8	1.44[13]	7024.7	1.76[13]			7006.1	6.04[12]		
$(^2D)^3D_3$	7935.0	2.27[13]					7030.4	2.25[13]		
$(^2D)^1D_2$	7942.6	1.32[13]	7056.6	1.70[13]			7038.0	1.20[14]		
$(^2D)^3P_0$			7093.5	7.18[13]						
$(^2P)^3P_1$	7982.9	2.67[11]	7096.8	1.17[13]	7930.6	2.64[13]	7078.2	5.87[13]	6171.9	3.36[9]
$(^2P)^3P_2$	8852.9	9.86[10]	7966.9	1.32[13]			7948.3	1.41[13]		
$(^2P)^1P_1$	8860.1	1.03[11]	7974.1	3.03[12]	8807.9	7.53[10]	7955.5	3.04[13]	7049.2	9.53[13]
					W^{66+}					
$(^4S)^5S_2$	8643.0	1.10[14]	7244.7	1.19[7]			7225.7	2.16[9]		
$(^4S)^3S_1$	8652.2	1.83[14]	7253.9	8.20[9]	8591.4	7.13[13]	7234.9	1.51[5]	5811.1	1.13[6]
$(^2D)^3D_1$	10037.2	4.68[13]	8638.8	1.85[14]	9976.4	2.11[11]	8619.9	3.73[13]	7196.0	3.79[9]
$(^2D)^3D_2$	10024.8	2.24[13]	8626.4	2.91[13]			8607.5	9.58[12]		
$(^2D)^3D_3$	10049.6	3.91[13]					8632.3	3.70[13]		
$(^2D)^1D_2$	10058.5	2.14[13]	8660.2	2.73[13]			8641.2	1.95[14]		
$(^2P)^3P_0$			8704.4	1.17[14]						
$(^2P)^3P_1$	10106.2	2.44[11]	8707.9	1.91[13]	10045.5	4.26[13]	8688.9	9.59[13]	7259.5	1.70[9]
$(^2P)^3P_2$	11489.2	5.51[10]	10090.9	2.50[13]			10072.0	2.58[13]		
$(^2P)^1P_1$	11497.7	7.98[10]	10099.4	6.28[12]	11436.9	4.25[10]	10080.4	4.99[13]	8656.6	1.54[14]
					Au^{71+}					
$(^4S)^5S_2$	9866.3	1.54[14]	7969.9	4.04[7]			7951.1	1.52[9]		
$(^4S)^3S_1$	9876.3	2.56[14]	7979.9	6.26[9]	9808.1	9.98[13]	7961.1	2.35[7]	6034.2	5.13[5]
$(^2D)^3D_1$	11759.9	6.20[13]	9863.6	2.59[14]	11692.7	2.02[11]	9844.7	5.22[13]	7917.9	3.16[9]
$(^2D)^3D_2$	11746.4	2.97[13]	9850.0	4.09[13]			9831.2	1.30[13]		
$(^2D)^3D_3$	11771.2	5.42[13]					9855.9	5.17[13]		
$(^2D)^1D_2$	11781.2	2.93[13]	9884.8	3.76[13]			9865.9	2.73[14]		
$(^2D)^3P_0$			9934.8	1.62[14]						
$(^2P)^3P_1$	11834.7	2.33[11]	9938.4	2.66[13]	11767.5	5.77[13]	9919.5	1.34[14]	7992.6	9.64[8]
$(^2P)^3P_2$	13717.6	4.53[10]	11821.2	3.60[13]			11802.4	3.67[13]		
$(^2P)^1P_1$	13727.0	7.03[10]	11830.6	9.45[12]	13659.8	3.44[10]	11811.7	6.83[13]	9884.9	2.14[14]

strengths in the low- and high-Z regions. However, the $2p^3(^2D)3s\ ^3D_3$ state suffers level crossings involving states from the $2p^3 3d$ configuration at $Z \sim 52$. These level-crossing interactions introduce a sharp discontinuity in oscillator strength at $Z \sim 54$. At $Z \sim 54$, the oscillator strength is reduced by more than four orders of magnitude (see Fig. 3). The $2p^3 3s\ ^3P_1$ and $2p^4\ ^3P_2$ states approach the $2p^1_{1/2}2p^2_{3/2}$ (0) $3s$ $J=1$ and $2p^2_{1/2}2p^2_{3/2}$ (2) $J=2$ j-j coupling states, respectively, at high Z. The $2p^3 3s\ ^3P_1 - 2p^4\ ^3P_2$ transition starts out as a medium-strong transition at low Z and shows strong irregularities for $44 \leq Z \leq 50$ due to the level-crossing interactions with $2p^3(^4S)3d\ ^5D_1$ and $2p^3(^2D)3d\ ^3D_1$ states (see Table III). At high Z, this transition becomes rather weak because the transition involves spectator core changing (Fig. 4). The $2p^3(^2P)3s\ ^1P_1$ state approaches the $2p^0_{1/2}2p^3_{3/2}3s$ $J=1$ state in the high-Z limit. Thus, the $2p^3(^2P)3s\ ^1P_1 - 2p^4\ ^3P_2$ transition is $E1$-forbidden in both the low- and high-Z regions. The oscillator strengths are very small for low- and high-Z ions. For mid-Z ions, the behavior of the oscillator strength is strongly influenced by spin-orbit mixing and level-crossing interactions. The oscillator strength suffers numerous discontinuities along the isoelectronic sequence due to the many level-crossing interactions involving $2p^3(^2P)3s\ ^1P_1$ and $2p^3 3d$ states (see Table III and Fig. 6). Similar irregularities have also been observed for many other transitions. At the region of strong cancellation, the theoretical results may strongly depend on the atomic model. A factor of 2 to 3 variation in rates is not unexpected. However, the Z dependence of the oscillator strength is believed to be qualitatively correct.

For comparison, results from nonrelativistic multiconfiguration Hartree-Fock calculations (MCHF) are

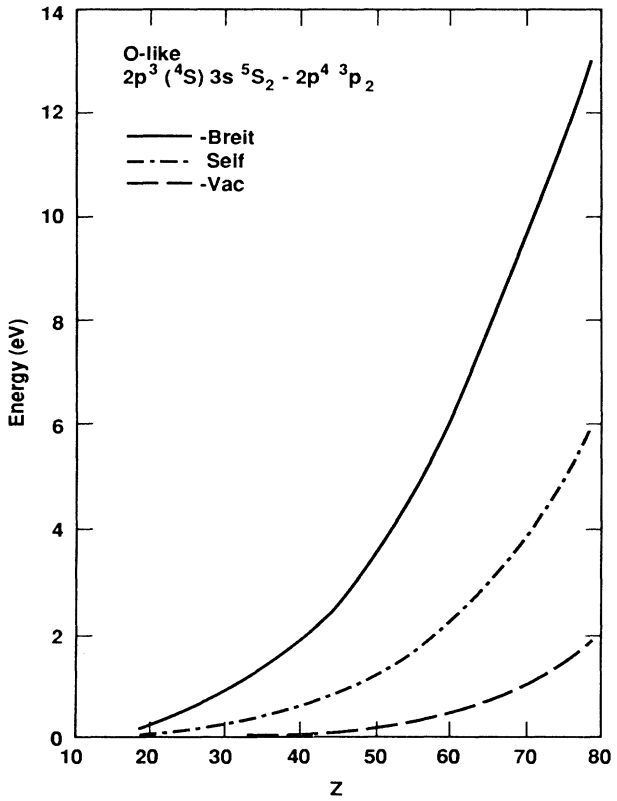

FIG. 1. Contributions of the Breit interaction and QED corrections to the $2p^3(^4S)3s\ ^5S_2-2p^4\ ^3P_2$ transition energy, as functions of atomic number. The solid curve pertains to the Breit interaction, the dash-dotted curve represents the self-energy correction, and the dashed curve indicates contributions from vacuum polarization.

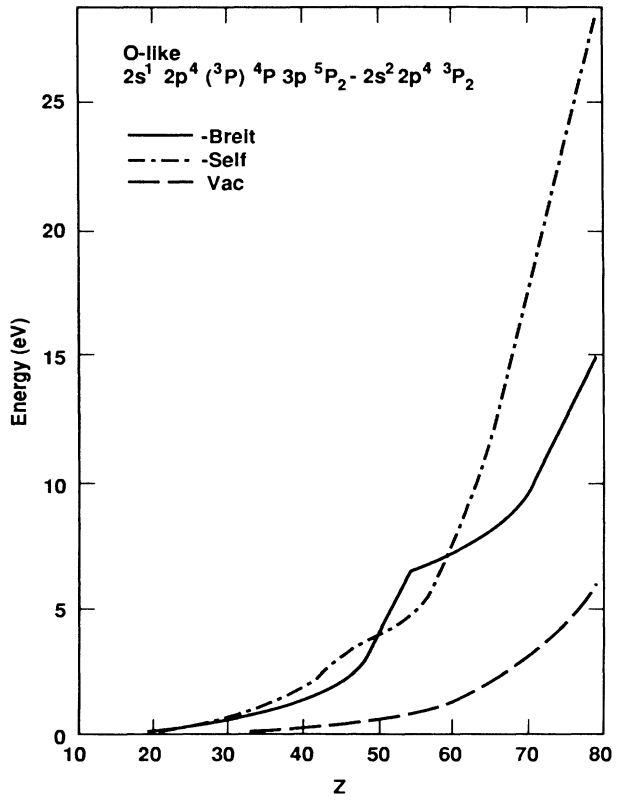

FIG. 2. Contributions of the Breit interaction and QED corrections to the $2s^12p^4(^3P)^4P3p\ ^5P_2-2s^22p^4\ ^3P_2$ transition energy. The legends are the same as in Fig. 1.

TABLE II. Lowest $J=0$ odd levels in the $2l^{-1}3l'$ complex of the oxygen isoelectronic sequence. The levels are arranged in ascending order in energy.

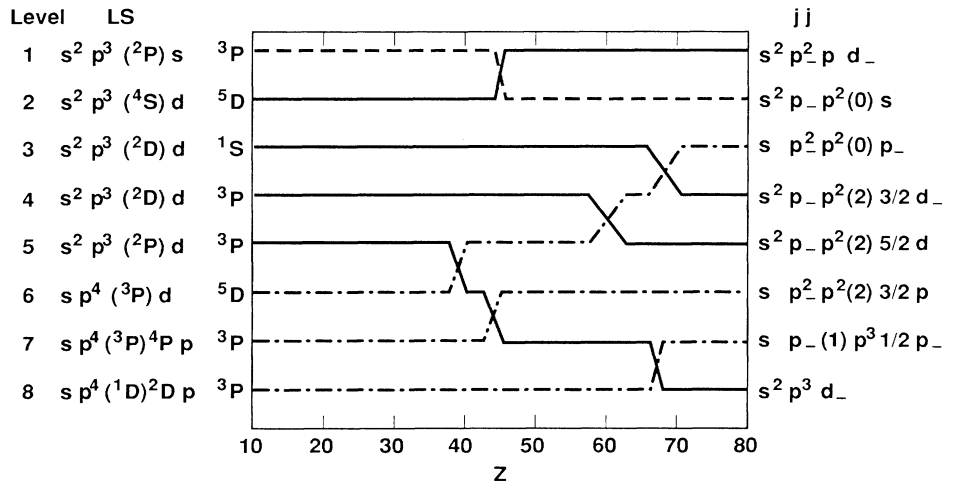

TABLE III. Lowest $J=1$ odd levels in the $2l^{-1}3l'$ complex of the oxygen isoelectronic sequence. The levels are arranged in ascending order in energy.

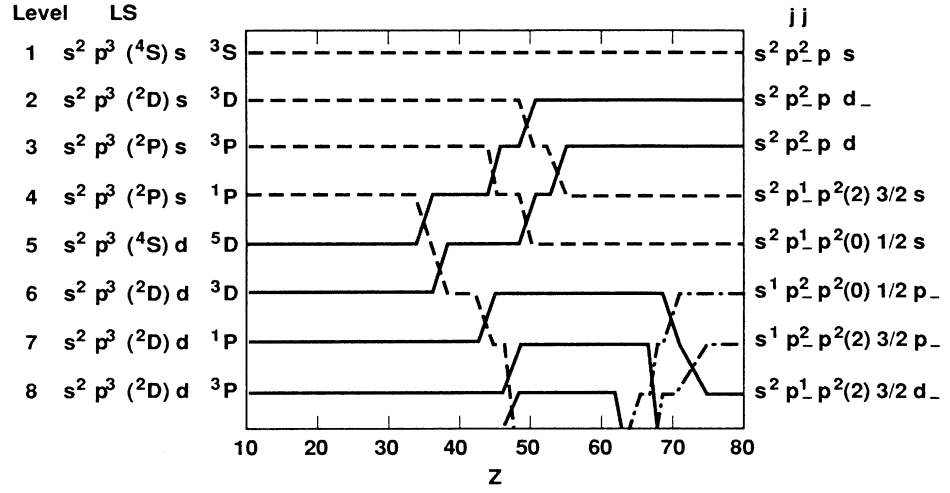

displayed in Figs. 3–5. These MCHF values were obtained by repeating the MCDF calculations with the velocity of light increased one thousandfold to simulate the nonrelativistic limit.[9] The oscillator strengths from the MCHF calculations exhibit regular behavior along the isoelectronic sequence. The oscillator strengths from the MCHF method differ from the relativistic values by as much as an order of magnitude for ions in the region involving level crossings. For transitions which are $E1$ forbidden at high Z but allowed at low Z, it is seen that the effects of relativity can reduce the oscillator strength by orders of magnitude for heavy ions.

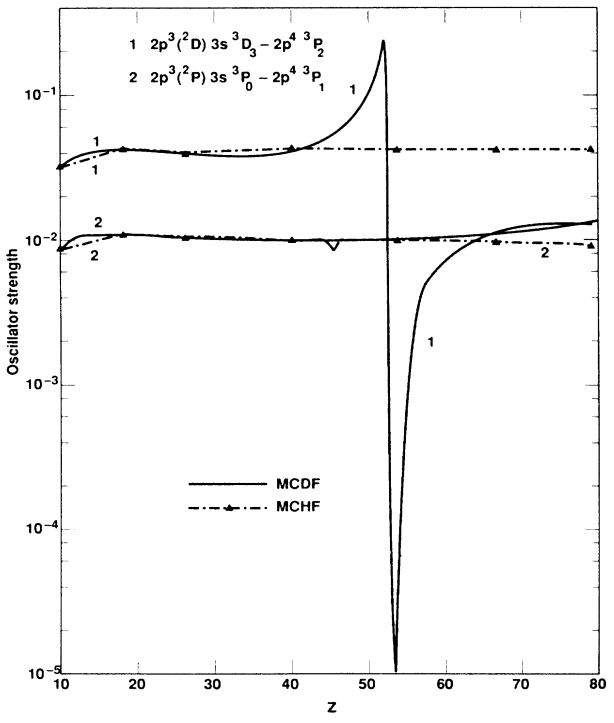

FIG. 3. Absorption oscillator strengths as functions of atomic number. The solid curves represent the results from the MCDF calculations. The triangles indicate the nonrelativistic MCHF values.

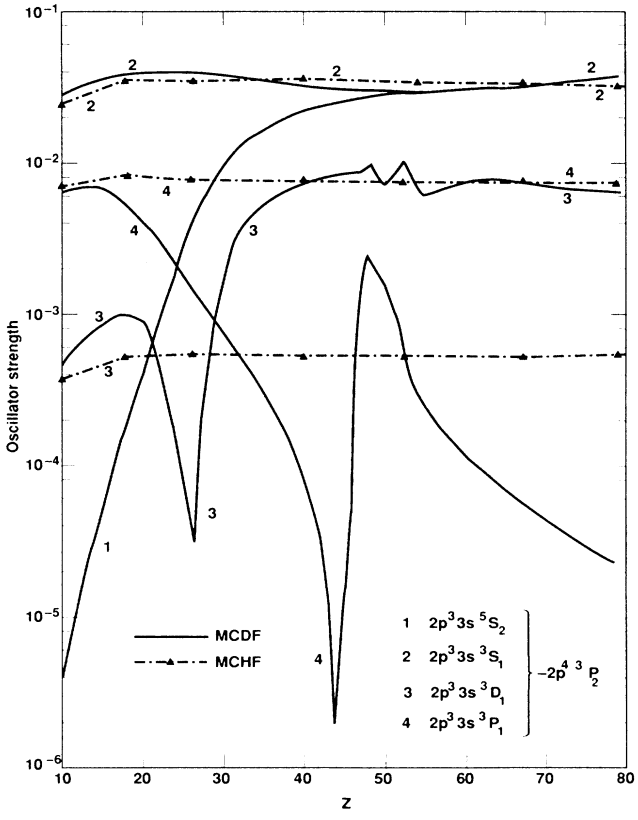

FIG. 4. Absorption oscillator strengths as functions of atomic number. The legends are the same as in Fig. 3.

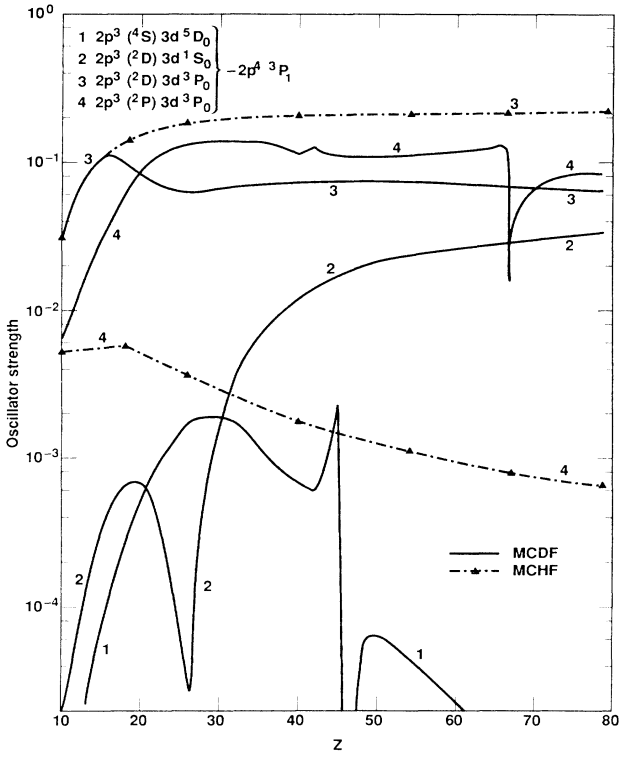

FIG. 5. Absorption oscillator strengths as functions of atomic number. The legends are the same as in Fig. 3.

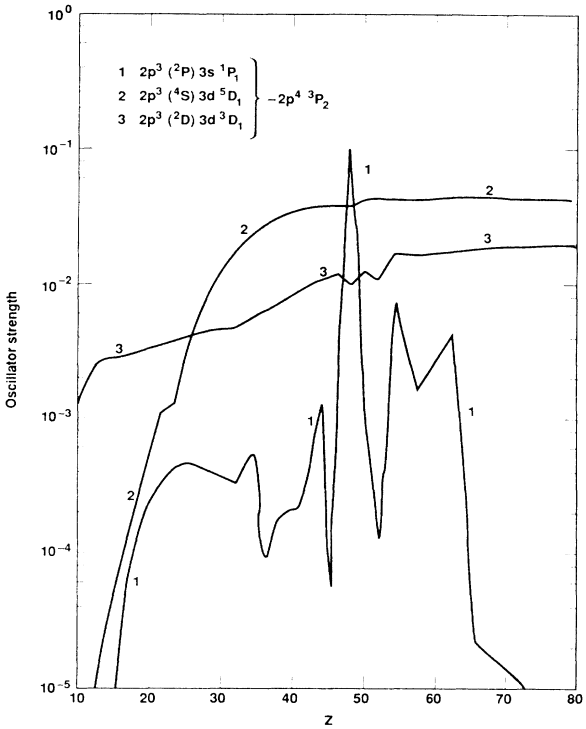

FIG. 6. Absorption oscillator strengths as functions of atomic number.

V. CONCLUSIONS

Energies and oscillator strengths for the $n=3$ and 2 electric dipole transitions in ions of the oxygen isoelectronic sequence have been calculated using the MCDF method. Both the effects of relativity and configuration interaction have been found to be important for medium and highly charged ions. To obtain accurate wavelengths, it is essential to include higher-order effects such as the Breit interaction and QED corrections. The systematic trends of the oscillator strengths are strongly perturbed by the effects of spin-orbit mixing and level crossings. Numerous irregularities in the oscillator strengths along the isoelectronic sequence can occur for many transitions in 10 to 60 times ionized atoms because of the level-crossing interaction. The usefulness of isoelectronic sequence regularities for organizing f-value data pertaining to complex open-shell ions is severely hampered by the frequent occurrence of these irregularities.

ACKNOWLEDGMENTS

We sincerely thank Mei Chi Chen for her expert computational assistance. We are grateful to William F. Ballhaus, Jr., Director of the NASA Ames Research Center (ARC), for permission to use the computational facilities of the center, and thank the ARC Computational Chemistry and Aerothermodynamics Branch, particularly David M. Cooper, for their hospitality. This research was performed in part under the auspices of the U.S. Department of Energy by the Lawrence Livermore National Laboratory under Contract No. W-7405-ENG-48. At the University of Oregon this work was supported in part by the National Science Foundation through Grant No. PHY-8516788 and by the U.S. Air Force Office of Scientific Research under Grant No. AFOSR-87-0026.

[1]W. L. Wiese and A. W. Weiss, Phys. Rev. **175**, 50 (1968).
[2]A. W. Weiss, in *Beam-Foil Spectroscopy*, edited by I. A. Sellin and D. J. Pegg (Plenum, New York, 1976).
[3]K. T. Cheng and Y. K. Kim, J. Opt. Soc. Am. **69**, 125 (1979).
[4]A. Farrag, E. Luc-Koenig, and J. Sinzelle, J. Phys. B **13**, 3939 (1980); J. Phys. B **14**, 3325 (1981).
[5]K. N. Huang, Y. K. Kim, K. T. Cheng, and J. P. Desclaux, At. Data Nucl. Data Tables **28**, 355 (1983).
[6]J. P. Declaux and Y. K. Kim, Phys. Rev. Lett. **36**, 139 (1976).
[7]K. N. Huang, At. Data Nucl. Data Tables **30**, 313 (1984); **32**, 503 (1985); **34**, 1 (1986).
[8]E. Biemont and J. E. Hansen, At. Data Nucl. Data Tables **37**, 1 (1987).
[9]I. P. Grant *et al.*, Comput. Phys. Commun. **21**, 207 (1980).

[10]M. H. Chen, Phys. Rev. A **31**, 1449 (1985).
[11]I. P. Grant, J. Phys. B **7**, 1458 (1974).
[12]J. Hata and I. P. Grant, J. Phys. B **14**, 2111 (1981).
[13]I. I. Sobel'man, *Introduction to the Theory of Atomic Spectra* (Pergamon, New York, 1972).
[14]M. H. Chen and B. Crasemann, At. Data Nucl. Data Tables (to be published).
[15]W. R. Johnson and K. T. Cheng, in *Atomic Inner-Shell Physics*, edited by B. Crasemann (Plenum, New York, 1985), p. 3.
[16]P. J. Mohr, Ann. Phys. **88**, 52 (1974); Phys. Rev. Lett. **34**, 1050 (1975); Phys. Rev. A **26**, 2338 (1982).
[17]M. H. Chen, Nucl. Instrum. Methods B **43**, 366 (1989).